HYDRAULIC ASPECTS IN DESIGN AND OPERATION OF AXIAL-FLOW PUMPS

Helmut Jaberg
Institute for Hydraulic Machinery, Graz, Austria

Keywords : Axial flow pumps, Cavitation, Characteristic curve, Diffuser, Diffusion factor, Impeller, Theoretic head

Contents

Summary

The best machines for handling high capacities at small head differences are propeller pumps. The flow conditions in this pump type are explained in detail, and it is pointed out why, in particular propeller pumps, they require such exacting quality demands regarding design and manufacturing.

This article is, above all, addressed to consultants and operators of pumping stations with propeller pumps and is intended to provide a comprehensible description of

modern propeller pump technology.

1. Introduction

Consultants and operators specifications of pumping stations to the pump manufacturer often require that the pump lifts large capacities over low geodetic head differences. Examples of this kind of application are bucket elevators, stormwater and flood-water pumping stations, cooling water supply systems, and sewage treatment plants. Suitable pumps for these requirements are axial-flow pumps.

The ratio of inlet and outlet radii of the pump impeller is primarily determined by the total head required: the higher the head, the larger the ratio of radii. Given the low heads resulting from the applications listed above the ratio of the radii approaches 1; this calls for an axial design where the head is achieved by reaction only. In principle, this requirement could also be met by using radial or mixed-flow impellers; however, a good efficiency and a technically reasonable pump size for high volume capacities and low heads can only be achieved with axial pumps. One criterion for the design is the specific speed n_q, which is calculated by a geometrically similar conversion of a certain pump into one with a capacity of 1 $m^3 s^{-1}$ and a head of 1 m. According to experience, pumps with low specific speeds are equipped with radial impellers, medium specific speeds require mixed-flow impellers, and high-specific-speeds above $n_q = 150$ are achieved with axial impellers.

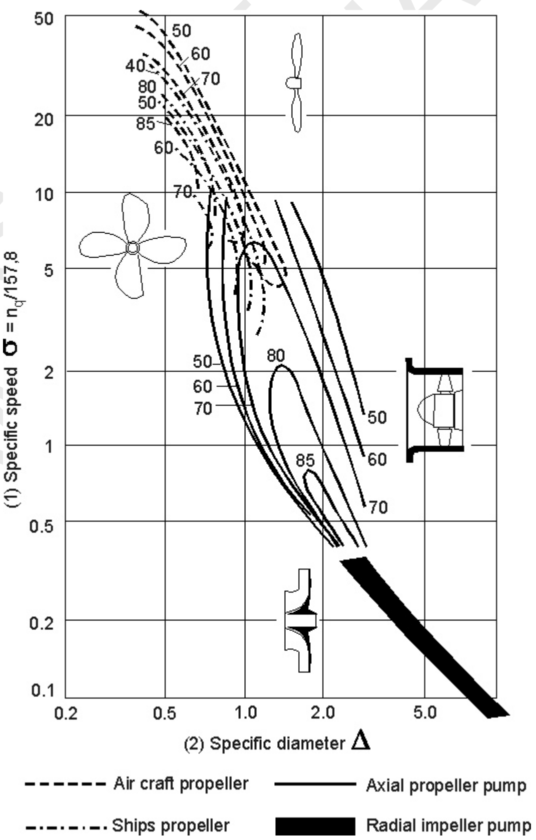

Figure 1. Cordier diagram (numerical values = η in %).

Cordier (1955) succeeded in providing a similarity-true diagram of the feasible efficiencies as a function of the speed and a dimensionless diameter coefficient. The Cordier diagram (Figure 1) assigns different impeller designs to their specific speed and thus indicates the peak efficiency that can be obtained. This Cordier diagram allows a comparative study of all turbomachinery from low speed radial impellers via axial pumps to ship and air propellers.

2. Flows in Axial-flow Pumps

The impellers and diffuser of axial-flow pumps consist of vanes whose profiles are derived from airfoils. Thus, it can be ensured that the flow reaction required for generating the energy conversion is performed with the highest benefit possible. High-speed propeller pumps with $n_q > 300$ are equipped with just two impeller blades; with decreasing specific speed n_q, the number of blades increases up to approximately eight at $n_q = 150$.

The cascade flow of propeller vanes shows a number of peculiarities which make the vanes very sensitive in terms of hydraulics and will therefore be explained in detail. In order to guarantee a high product quality, in spite of these difficulties, KSB carried out studies in their in-house research center, which have produced details about the flow in vane cascades of propeller pumps and thus provide reliable knowledge in this demanding field.

2.1. Vane Cascade Flow and Characteristic Curve

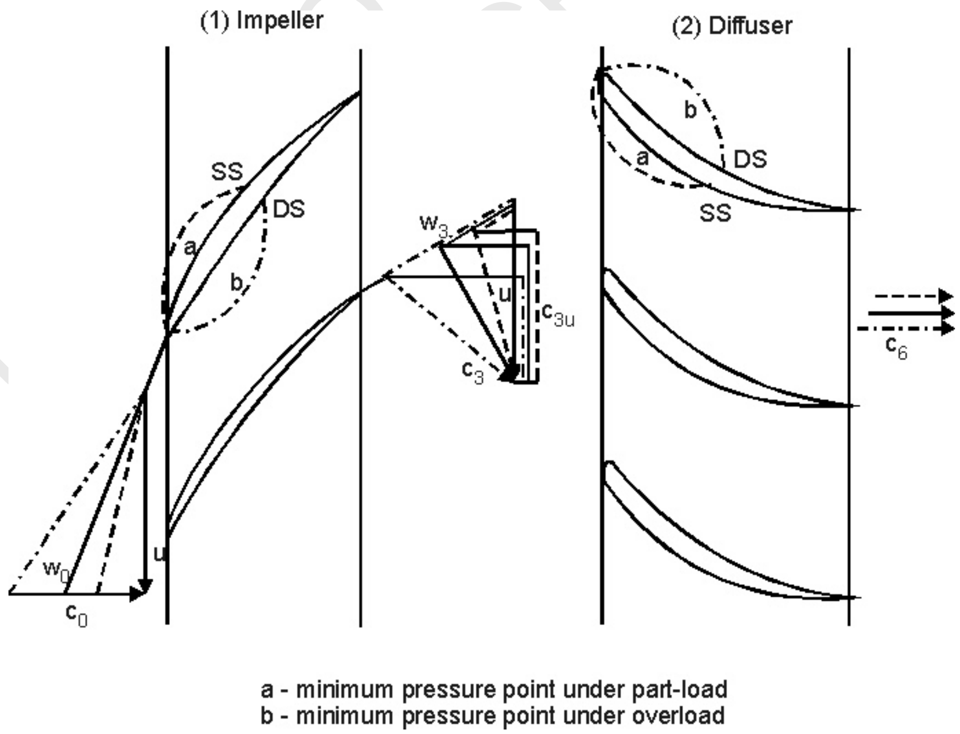

Figure 2. Cascade flow at design point (___), under part load (-----) and overload conditions ( ).

In axial propeller pumps the flow approximately moves along a coaxial cylindrical section. In the impeller the flow is redirected, which results in a pressure increase, since it acts like a divergent channel with energy supply. The medium handled enters the impeller in axial direction and leaves it, as illustrated in Figure 2, with an angular momentum and thus a higher absolute and lower relative velocity. By a second redirection in axial direction in the diffuser and, consequently, further deceleration, the diffuser also contributes to the pressure build-up or head generation.

In accordance with the curvature and profile of the impeller and diffuser vanes a low-pressure area develops on their convex side and a high-pressure area on their concave side. Therefore, a distinction is made between the suction side SS and the pressure side DS of the vane.

If the capacity is reduced, i.e. if the duty point is shifted towards part load, the inlet velocity c_o decreases, with the peripheral velocity u remaining unchanged, and the flow approaches the vane at a flatter angle (see Figure 2). On the vane suction side minimum pressure regions develop in the area which is characterized by low-pressure and may lead to cavitation problems.

Since the flow has to move from an extremely low pressure area to a high pressure area, flow separations may occur along the flow path. The outlet angle of the flow remains more or less the same, even for part-load conditions, but the height of the velocity triangle (see Figure 2) diminishes. This results in a flatter inlet angle into the diffuser, which - similar to the impeller - develops minimum pressure regions on its suction side, resulting in a potential risk of flow separation. Another consequence of the smaller axial velocity downstream of the impeller is an increase in the peripheral component of the absolute velocity at the impeller outlet, causing an increase in the head, as shown below.

If the capacity is increased, i.e. when operating in the overload area, the axial inlet velocity rises, and the impeller is approached at a steeper angle than at design point. This case is referred to as a *suction side impact*. Here, the minimum pressure peaks develop on the pressure side DS, which may also be subject to cavitation, even though not to the same extent as the suction side with its lower pressures. Due to the axial velocity increase, the axial velocity at the impeller outlet and the absolute angle increase. Consequently, the diffuser is also approached with a suction side shock - with consequences similar to those for the impeller. The peripheral component of the absolute velocity decreases, and, therefore, the head is reduced.

Since flow rate, beyond the design point, is characterized by increased losses, the efficiency decreases both at overload and at part-load conditions. In the case of axial propellers with relatively low heads, these losses have considerable magnitude and, in contrast to radial pumps, lead to a steeper efficiency curve over the capacity.

The characteristic curves, also called throttling curves, for axial propellers are relatively steep, which is a result of the flat outlet angles (Stepanoff 1959). Towards part-load, all characteristic curves H(Q) of Figure 3 show a saddle shape, since, in case of this capacity, the flow in the flow channels stalls. Even at a slightly higher capacity, the so-called *operating limit*, the phenomenon of rotating stall occurs: the flow stalls at the suction side of one vane and partly blocks the flow channel. Due to this blockage, the flow is forced into the two adjacent channels, which means that the adjacent channel in the direction of rotation is approached at a steeper angle, whereas the flow into the adjacent channel opposite to the direction of circulation is even flatter. Consequently, the flow in this channel will stall next, which, in turn, makes the channel flow stalled previously steeper, and thus results in re-establishing contact in this channel. It also causes a latter inlet flow angle to the next channel opposite to the direction of rotation followed by a stall. The stall thus moves in the opposite direction to the impeller rotation and is therefore called rotating stall. Rotating stall is of major concern, since it may cause undesirable vibrations and, in extreme cases, even a vane failure. This has to be taken into consideration for stability design of the vane. Rotating stall is also found in radial pumps, where it is considered to be the cause of unstable characteristic curves.

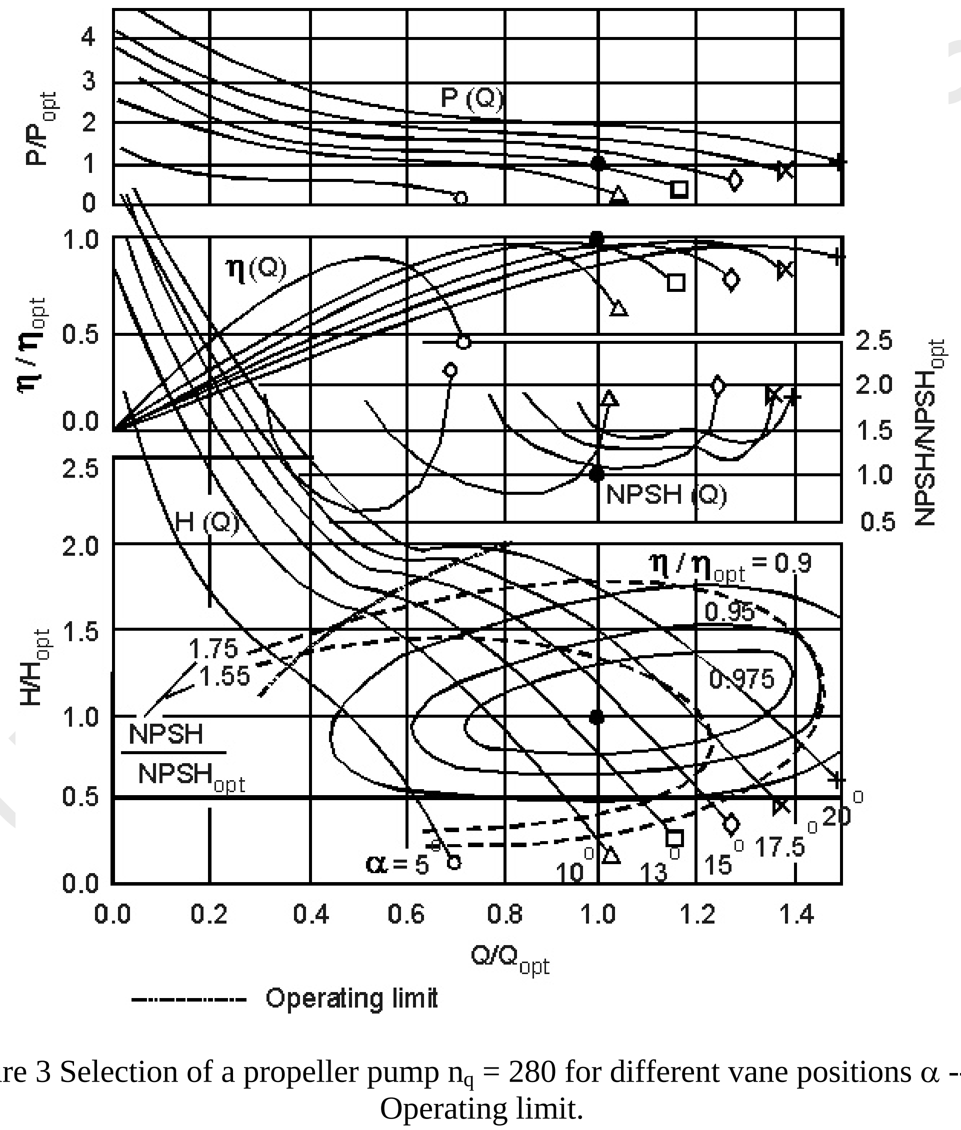

Figure 3 Selection of a propeller pump n_q = 280 for different vane positions α ---.--- Operating limit.

When the capacity is further reduced, the characteristic curve passes the said "saddle" and again rises steeply toward lower flow. This rise results from the appearance of part-load and interchange vortices upstream and/or downstream of the diffuser, where the medium handled leaves the impeller and re-enters it on a different diameter. Thus energy is added several times to part of the medium, and the characteristic curve rises in this area since the repeated supply of energy exceeds the losses caused by poor inlet triangles as described above. In addition, the flow no longer moves in the axial direction, but moves from a smaller radius at the inlet to a larger one at the outlet and thus absorbs more energy. However, this phenomenon goes hand-in-hand with a considerable increase in power consumption, i.e. the above-mentioned steep efficiency curve over the capacity according to Figure 3 develops. The energy input P(Q) of the hydraulics is illustrated in Figure 3 and shows the decline of energy input with increasing flow, which is well-known for high-specific speed pumps. The large increase in power consumption at small capacities is a significant phenomena of high specific-speed pumps. This is in contrast to the power input of low specific-speed pumps, where the power input rises with increasing capacity. The reason for the difference can be found in the recirculation effects described as they constitute only a fraction of the total energy conversion in low specific-speed pumps, where the power input rises with increasing capacity. The reason for the difference can be found in the recirculation effects described as they constitute only a fraction of the total energy conversion in low specific-speed pumps. At n_q = 100 the power consumption over the capacity is found to be approximately constant.

The total head is determined from the difference of the total pressures $p_{tot,D}$ and $p_{tot,S}$ at the discharge and suction side of the pump, divided by the density ρ of the medium handled and the gravitational constant g:

$$H = \frac{p_{tot,D} - p_{totS}}{\rho . g} \qquad (1)$$

It results from the energy added in the hydraulic stage, which according to Euler's turbomachinery equation can be written as theoretic head

$$H_{th} = \frac{1}{g}\left(u.c_{3u} - u.c_{0u}\right) \qquad (2)$$

and has to be reduced by the losses caused by friction, poor inlet flow conditions, and blockage due to guide vane finite thickness:

$$H = H_{th} - H_v = H_{th} \ \ \eta_i \qquad (3)$$

It follows from Eeuler's equation that the head is proportional to the peripheral component of the absolute velocity downstream of the impeller c_{3u}, which rises with decreasing capacity, as discussed earlier. If necessary, a prerotation at the inlet, c_{0u}, must be subtracted. Depending on the sign of the pre-rotation component this may increase or reduce the total head. Capacity control by pre-rotation swirl adjustment of pumps is based on this effect (see: Section 4.2.5 Inlet Swirl Adjustment), below.

2.2. Sensitivity to Geometric Errors and Losses

As already mentioned, axial propeller pumps in particular are extremely sensitive to minor geometric errors or losses. In this section we will show that even minimum deviations from the specified geometry may shift the duty point considerably and lead to a marked change in head. Since axial pumps in general produce only low heads, any further loss will result in undesirable losses of efficiency and head.

Figure 4 illustrates the effect of a discharge angle reduced by just one degree. For three different capacity coefficients, φ corresponding to a dimensionless capacity the ratio of the theoretical heads H_{th} at a wrong discharge angle to those at a correct discharge angle H^*_{th} are plotted.

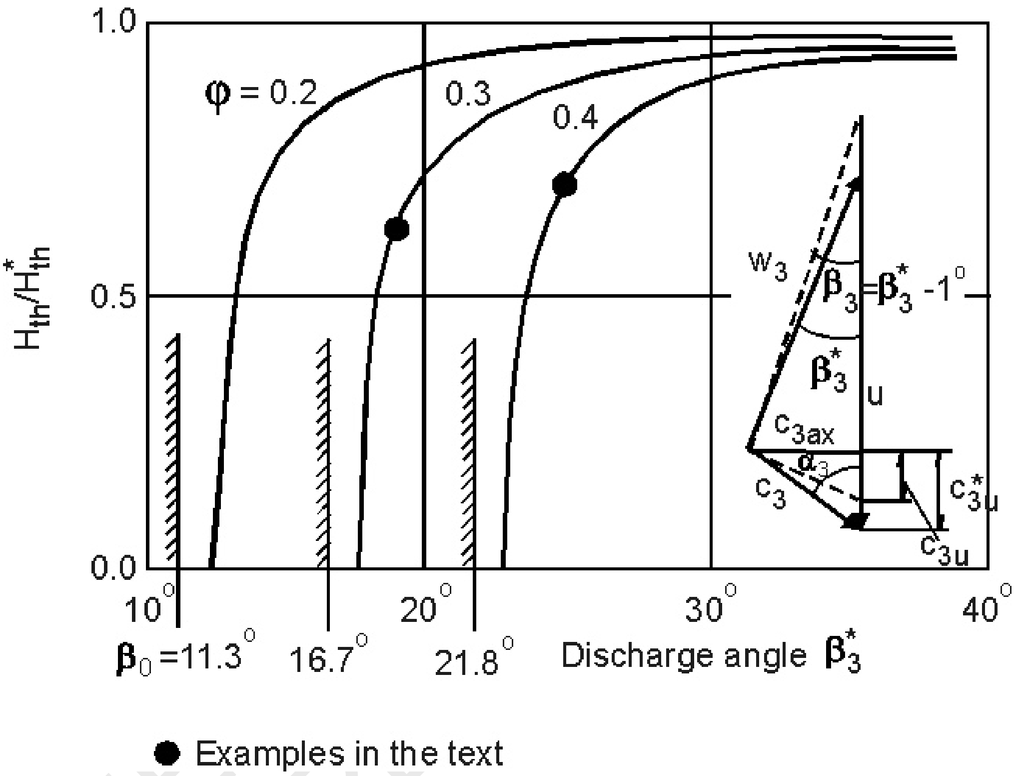

Figure 4. Sensitivity: change in the head H_{th} for a discharge angle deviating by one degree ($\beta_3 = \beta_3^* - 1°$) for different capacity coefficients φ or inlet flow angles β_0 (β_3^* = design discharge angle).

In addition, the inlet flow angles β_0 pertinent to each capacity coefficient φ are indicated. If the influences of boundary are neglected, the result is (Stepanoff 1959):

$$\frac{H_{th}}{H^*_{th}} = \frac{1-\varphi.\cot\beta_3}{1-\varphi.\cot\beta^*_3} \qquad (4)$$

Figure 4 shows that in case of major deviations, i.e. large β_3*, the ratio of the heads approaches 1, in other words: deviations in the discharge direction hardly affect the head at all. High-speed axial machines, in contrast, are characterized by slightly curved vanes with slight deviations, i.e. by small angles β_3*. In these areas the curves for the ratio of the heads are very steep, however, and assume values much smaller than 1. If we look, for instance, at a vane with the specific speed $n_q = 310$ and a capacity coefficient $\varphi = 0.3$, a discharge angle of 18 degrees is required at its outer diameter in case of an inlet flow angle of 16.7 degrees. If, due to manufacturing inaccuracies or other circumstances, a discharge angle of just 17 degrees is achieved, the head decreases by 37 per cent as compared to the design point. In the center cross section between hub and casing of the vane the capacity coefficient is $\varphi = 0.4$, which in the case of an inlet flow angle of 21.8 degrees requires a discharge angle of 25 degrees. Given an angular deviation of one degree the head loss as compared with designed value amounts to 28 per cent. If we keep in mind that an angular modification of just one degree already results in a considerable head loss, the significance of these accuracy requirements becomes evident.

The sensitivity of the vane to modifications of the inlet flow angle is illustrated in Figure 5, which shows the loss parabola of a propeller vane. Every flow profile results in certain profile losses, above all by friction and wrong inlet flow angles. If the inlet flow has an optimum angle, the loss curve reaches its minimum and the vane its optimum efficiency (Horlock 1967). However, if the loss parabola shifts, for instance, because of a slight modification of the vane curvature, an increase of the profile losses and, in our example, an efficiency loss of 2 per cent is the result for the initially optimal inlet flow angle. If the flow, in contrast, approaches the vane at the new angle with lowest loss coefficient, the result is a displacement of the optimum point to a capacity increased by 6 per cent. For the steep propeller pump characteristic curves (see Figure 3) this causes a considerable shift of the duty point towards a markedly higher specific-speed. In this case, too, the vane would no longer be suitable for the requirements of application.

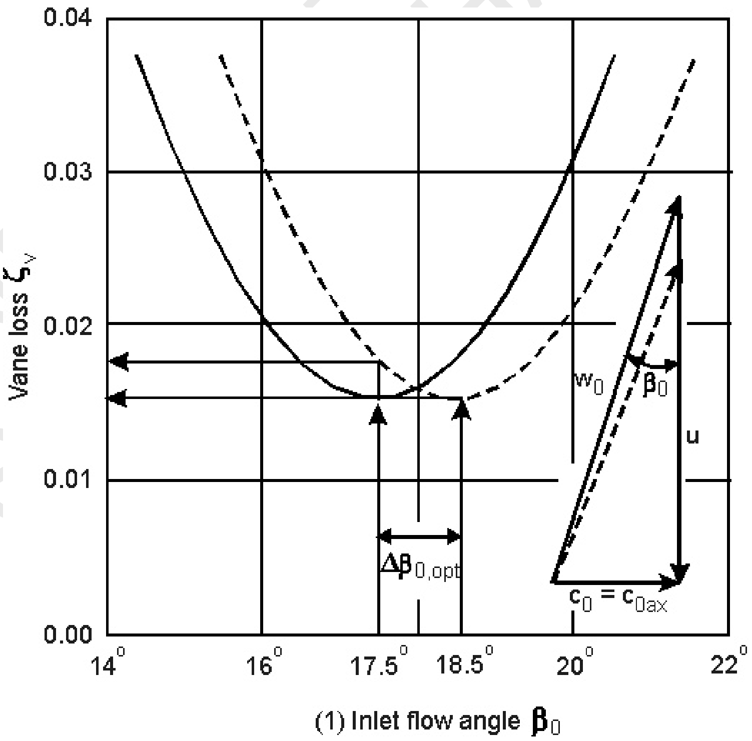

Figure 5. Sensitivity of inlet flow. Vane losses ζ_v of an optimum vane ( ) and a vane with a curvature deviating by one degree ( ) ($\Delta\beta_{0,Opt} = 1°$: $\Delta\eta = -2$ %-points or optimum point at $\Delta Q = +6\%$).

-
-
-

Bibliography and Suggestions for further study

Anspach E, Höhn W, Knapp P, Semler F (1987) Computer-aided evaluation of waterhammer protection in fluid flow system. KSB Technische Berichte, No. 21e, pp. 3-15.

Bauer G H (1982) Verlustbeiwerte von Rohrkrümmern (Loss coefficients of pipe elbows). KSB Interner Bericht.

Bernauer J, Stark M and Wittekindt W (1987) Improvement of propeller blades used for handling liquids containing fibrous solids. In: KSB Technische Berichte, No. 21e, pp. 16-21.

Bieniek K (1988) Submersible motors and wet-rotor motors for centrifugal pumps submerged in the fluid handled. KSB Technische Berichte, No. 23e, pp. 9-17.

Cordier O (1955) Ähnlichkeitsbedingungen für Strömungsmaschinen (Similarity conditions for turbomachinery). In: VDI-Berichte, No. 3, pp. 85-88.

Denton J D and Hirsch C (1981) Through flow calculations in axial turbomachines. AGARD AR 175.

Domm U, Rosemann P and Siekmann H (1973) Modelluntersuchung der Einlaufströmung einer groβen Kühlwasserpumpe (Model study of the inlet flow into a large cooling water pump). In: KSB Technische Berichte, No. 16, pp. 3-9.

Europump (ed.) (1974) NPSH bei Kreiselpumpen (NPSH in centrifugal pumps). Frankfurt/M: Maschinenbauverlag.

G. Penninger, H.Benigni, H.Jaberg (2005), New design of butterfly valves for modern pump-storage power plants, Hydro2005 Conference and exhibition, Villach,

Gehrer, A., Egger A., Riener J.(2002), Numerical and Experimental Investigation of the draft tube flow downstream of a bulb turbine, proceedings of the 21st IAHR Symposium on Hydraulic Machines and Systems, Lausanne,

Hergt P (1984) Kavitation in Kreiselpumpen (Cavitation in centrifugal pumps). In: KSB-Druckschrift 0383.051.

Holzenberger K (1989) Ermittlung des Drehmomentenverlaufs beim Anfahren von Kreiselpumpen mit Hilfe von Kennzahlen (Centrifugal pump starting torques). KSB Technische Berichte, No. 26, pp. 3-13.

Holzenberger K and Rau L (1988) Parameters for the selection of energy conserving control options for centrifugal pumps. In: KSB Techinsche Berichte, No. 24e, pp. 3-19.

Horlock J H (1967) Axialkompressoren (Axial compressors). Karlsruhe: Braun.

Jaberg H (1986) Der Zusammenhang NPSH-Laufraddurchmesser bei Axialpumpen (The relation between NPSH and impeller diameter for axial pumps). KSB Interner Bericht.

János VAD, Ferenc BENCZE, Helmut BENIGNI, Wolfgang GLAS and Helmut JABERG(2002), *Comparative Investigation On Axial Flowpump Rotors Of Free Vortex And Non-Free Vortex Design*, Periodica Polytechnica Ser. Mech. Eng. VOL. 46, NO. 2, PP. 107–116

Lewinsky-Kesslitz H P (1986) Estimating and avoiding waterhammer - a practical guide. KSB

Technische Berichte, No. 20e, 39-49.

Meusburger, P.(2009), Die 1D transiente numerische Simulation von modernen Hochdruck-Wasserkraftanlagen. Doctoral Thesis, University of Technology Graz,

Migod A and Siekmann H (1977) Einfluβ von Kühlverfahren und Zulaufbedingungen auf die Bauart von Kühlwasserpumpen für Wärmekraftwerke (Influences of the cooling method and inlet conditions on the design of cooling water pumps for thermal power stations). In: KSB Technische Berichte, No. 17, pp. 25-4.5.

National Aeronautics and Space Administration (NASA) (1965) Aerodynamic design of axial-flow-compressors, NASA SP-36.

Penninger, G., Benigni, H.(2006), Numerical simulation and design of spherical valves for modern pump storage power plants, 14th International Seminar on Hydropower Plants, Vienna,

Petermann H and Pfleiderer C (1964). Strömungsmaschinen (Turbomachinery). 3. Aufl. Berlin: Springer.

Pfleiderer C (1955) *Die Kreiselpumpen für Flüssigkeiten und Gase* (Centrifugal pumps for fluids and gases). Berlin: Springer.

Rau L (1983) Auslegung einer Axialpropellerhydraulik mit dem Rechenprogram AXOPT (Designing and axial propeller hydraulics by means of the AXOPT computing program). KSB Interner Bericht.

Saalfeld K (1954) Berechnung und Konstruktion von Propellerschaufeln (Calculation and construction of propeller blades). KSB Interner Bericht.

Stepanoff A H (1959) Radial-und Axialpumpen (Radial and axial pumps). 2nd edn. Berlin: Springer.

Stiefel W (1959) Betrachtungen zur Auslegung der Beschaufelung von axial durchströmten Verdichtern (Studies on the blading design of axial flow compressors). MTZ, No. 9, 340-346.

Strscheletzky M (1960) Gleichgewichtsformen der rotationssymmetrischen Strömungen mit konstantem Drall in geraden, zylindrischen Rotationshohlräumen (Forms of equilibrium of dynamically balanced flows with constant vortex in straight, cylindrical rotation cavities*).* In: Voith-Forschung und Konstruktion, No. 5, pp. 1-19.

Truckenbrodt E (1980) Fluidmechanik (Fluid Mechanics) Bd. 1. Berlin: Springer.